Published in final edited form as:
Nat Neurosci. 2008 September ; 11(9): 1100–1108. doi:10.1038/nn.2177.

Interhemispheric correlations of slow spontaneous neuronal fluctuations revealed in human sensory cortex

Yuval Nir[1], **Roy Mukamel**[2], **Ilan Dinstein**[3], **Eran Privman**[4], **Michal Harel**[1], **Lior Fisch**[1], **Hagar Gelbard-Sagiv**[1], **Svetlana Kipervasser**[5,6], **Fani Andelman**[7], **Miri Y Neufeld**[5,6], **Uri Kramer**[5,7], **Amos Arieli**[1], **Itzhak Fried**[2,5,7], and **Rafael Malach**[1]

1 *Department of Neurobiology, Weizmann Institute of Science, 240 Herzl Street, Rehovot 76100, Israel*

2 *Division of Neurosurgery, David Geffen School of Medicine, and Semel Institute for Neuroscience and Human Behavior, University of California Los Angeles, Los Angeles, California 90095, USA*

3 *Center for Neural Science, New York University, 4 Washington Place, New York, New York 10003, USA*

4 *School of Computer Science, Sackler Faculty of Exact Sciences, Tel Aviv University, Tel Aviv 69978, Israel*

5 *Sackler School of Medicine, Tel Aviv University, Tel Aviv 69978, Israel*

6 *Electroencephalography and Epilepsy Unit, Department of Neurology, 6 Weizmann Street, Tel Aviv 64239, Israel*

7 *Functional Neurosurgery Unit, Tel Aviv Medical Center, 6 Weizmann Street, Tel Aviv 64239, Israel*

Abstract

Animal studies have shown robust electrophysiological activity in the sensory cortex in the absence of stimuli or tasks. Similarly, recent human functional magnetic resonance imaging (fMRI) revealed widespread, spontaneously emerging cortical fluctuations. However, it is unknown what neuronal dynamics underlie this spontaneous activity in the human brain. Here we studied this issue by combining bilateral single-unit, local field potentials (LFPs) and intracranial electrocorticography (ECoG) recordings in individuals undergoing clinical monitoring. We found slow (<0.1 Hz, following 1/*f*-like profiles) spontaneous fluctuations of neuronal activity with significant interhemispheric correlations. These fluctuations were evident mainly in neuronal firing rates and in gamma (40–100 Hz) LFP power modulations. Notably, the interhemispheric correlations were enhanced during rapid eye movement and stage 2 sleep. Multiple intracranial ECoG recordings revealed clear selectivity for functional networks in the spontaneous gamma LFP power modulations. Our results point to slow spontaneous modulations in firing rate and gamma LFP as the likely correlates of spontaneous fMRI fluctuations in the human sensory cortex.

The neuronal events occurring in the sensory cortex when no stimulus is presented are not well understood. Contrary to traditional feed-forward models of information processing, a growing body of single-unit, LFP, electroencephalography (EEG), and optical imaging data point to robust levels of spontaneous neuronal activity in sensory areas of the mammalian cortex[1–7]. The modulation of such spontaneous neuronal activity can occur on very slow time scales[8,9]. These robust spontaneous waves pose a challenge for models linking neuronal activity and sensory perception[10,11], namely in explaining how the brain distinguishes between spontaneous events and vivid sensory percepts. One possibility is that the precise neuronal dynamics differ substantially between spontaneous and sensory-evoked conditions. This

Correspondence should be addressed to R.M. (rafi.malach@weizmann.ac.il).

possibility is shown in the schematic models in Figure 1. Such dynamic differences may be missed in fMRI measurements because of the sluggish nature of the hemodynamic response (Fig. 1).

In the presence of uncorrelated noise, neuronal events with distinct dynamics are expected to differ in the spectral profiles of their firing-rate correlations across hemispheres (Fig. 1). High-amplitude transient neuronal activity would give rise to correlations at both low and high modulation frequencies, generating a relatively flat spectral correlation profile (model 1; Fig. 1), whereas low-amplitude sustained neuronal activity would give rise predominantly to correlations at low frequencies (model 2). Here we report the finding of correlated spontaneous fluctuations in low-frequency firing-rate modulations and gamma LFP power across hemispheres. We further show that the neuronal dynamics underlying these spontaneous fluctuations are clearly compatible with model 2, whereas the sensory-evoked correlations are more compatible with model 1.

A major concern in studying spontaneous signals is their possible contamination by noise sources, as no time-locked averaging is possible for such signals. To overcome this problem, we focused on two major defining characteristics of spontaneous brain activity, as also reported by fMRI studies: their tendency to be correlated across hemispheres[12–21], and their neuroanatomical selectivity[12–21]—that is, such fluctuations are not global, and distinct functional systems are often decorrelated. To assess these characteristics with electrophysiological measures, we used two rare sets of bihemispheric recordings obtained in the auditory cortex of individuals undergoing presurgical clinical testing. These data consisted of extracellular single-unit and LFP recordings obtained from depth electrodes in three individuals and subdural surface ECoG recordings from two other individuals (see Supplementary Table 1 online for details and Fig. 2a for bilateral auditory electrode locations in extracellular data). We focused on inter-hemispheric correlations as our marker for genuine spontaneous activity. Finally, by comparing intracranial ECoG recordings from the auditory cortex with many other recording sites in the same individuals, we verified the anatomical selectivity of the spontaneous neuronal activity.

RESULTS

Firing-rate and gamma LFP power modulations

We recorded single-unit activity and LFPs bilaterally from depth electrodes placed in the auditory cortex during wakeful rest and sleep (Fig. 2). We first focused on single-unit data, which were recorded in two individuals during silent wakeful rest and during pure-tone and random-chord stimulation[22] (n = 38 and 50, respectively, with a mean firing rate of 5.3 and 4.9 spikes s^{-1} during rest). We compared the firing-rate modulations of the auditory cortex during rest across hemispheres as follows. Firing-rate modulations were minimally smoothed (with a Gaussian with full width at half maximum (FWHM) of 5 ms) and further filtered into three frequency bands: slow (<0.1 Hz), medium (0.1–1 Hz) and fast (>1 Hz). We provide here an example of this analysis (Fig. 2b) and a summary of bilateral spiking data in two subjects (Fig. 3a). We found robust firing-rate modulations during wakeful rest, which were correlated across the two hemispheres. These modulations in single-unit firing rates manifested the highest and most significant interhemispheric correlations at low temporal frequencies (r = 0.32, $P < 0.0005$).

We next examined LFPs that were recorded during periods of silent wakeful rest and audiovisual stimulation in five individuals. Periods of both rapid eye movement (REM) and stage 2 sleep were recorded over two nights for one of these individuals (Supplementary Table 1). Because coherence across large cortical distances during rest is often associated with the raw LFP and EEG and its low-frequency rhythms[23], we first checked whether the raw LFP

showed correlations across the two hemispheres. Notably, we did not find marked interhemispheric correlations at any frequency of the raw LFP (>1 Hz) during wakeful rest in the extracellular data (Supplementary Fig. 1 online).

An important dimension of the LFP signal is its band-limited power (BLP)[4], which is a measure of envelope amplitude changes of LFP oscillations at specific frequency bands. In contrast to the raw LFP, an examination of BLPs revealed robust interhemispheric correlations. We observed the strongest correlations in gamma (40–100 Hz) power changes, although power changes at lower (alpha/beta) frequency bands also showed some interhemispheric correlations (see Supplementary Fig. 1 for all frequency bands). To examine the frequency profiles of the correlations, we further filtered the gamma power modulations into slow, medium and fast frequencies. Similar to the firing-rate modulations, the interhemispheric correlations in gamma power were higher at low (<0.1 Hz) frequencies (example in Fig. 2c). A quantitative analysis across the entire dataset (Fig. 3b) confirmed the strong bias of interhemispheric correlations in gamma-power modulations toward low frequencies ($r = 0.43$, $P < 0.0005$).

The concurrent acquisition of spiking activity and LFP allowed us to directly compare the modulations in firing rate and gamma LFP power (Supplementary Fig. 2 online) and determine the relationship between firing rate and gamma LFP power in spontaneous activity during wakeful rest. Similar to the interhemispheric correlations, the correlations between spiking activity and gamma power were significantly higher at low-frequency modulations (one-way analysis of variance (ANOVA) on Fisher transformed correlation coefficients; $P < 0.0001$, $F > 17.34$ for modulation frequency).

To examine the extent to which the correlations depended on the subjects' wakefulness, we compared interhemispheric correlations in wakeful rest and sleep states. Correlations of spontaneous LFP gamma power markedly increased during sleep, in both stage 2 and REM (examples of increased interhemispheric correlations during sleep are shown in Fig. 2d,e). This increase was also evident in the overall dataset ($r = 0.58$ during REM, $r = 0.64$ during stage 2, $P < 0.0005$; Fig. 3c,d). A quantitative comparison of wakeful rest and sleep states and slow, medium and fast frequencies revealed higher interhemispheric correlations during sleep for slow (<0.1 Hz) fluctuations (two-way ANOVA on Fisher transformed correlation coefficients, $P < 0.0001$, $F > 7.62$ for state; $P < 0.0001$, $F > 52.3$ for frequency; no interaction). We evaluated the statistical significance for the various states and frequencies (Fig. 3) by comparing the interhemispheric correlation coefficients to corresponding null distributions generated by bootstrapping. A full description of all interhemispheric LFP and BLP correlations during wakefulness and sleep is available in Supplementary Figure 1.

Spontaneous activity is dominated by low frequencies

The results thus far suggest that correlations in spontaneous activity across hemispheres are mainly evident at low frequencies—that is, they support model 2 (Fig. 1). We examined whether a similar low-frequency bias is evident in the power spectrum of the local spontaneous activity. To that end, we first computed the autocorrelation of local activity (each auditory cortex on its own), as well as the interhemispheric cross-correlation, without filtering the activity into predefined frequency bands. The results provide an unbiased account of the slow (<0.1 Hz) nature of both the local and correlated spontaneous fluctuations (Fig. 4). We also computed the Fourier transforms of the autocorrelation function (power spectrum) and the cross-correlation function (cross-spectrum). The power spectra of spontaneous activity, both local and correlated across hemispheres, were strongly biased toward low frequencies, following a 1/*f*-like power distribution (Fig. 4, insets). Finally, we examined the possibility of consistent temporal asymmetry in interhemispheric correlations, but we did not find a significant bias during wakeful rest ($P = 1$, $n = 8$ sessions for spiking activity; $P = 1$, $n = 9$

sessions for gamma BLP) or during sleep ($P = 0.18$, $n = 35$ recording segments for gamma BLP).

Power-law spectra such as $1/f$ are also typical of natural sounds, so it could be argued that the 'spontaneous' fluctuations actually reflect auditory responses to uncontrolled ambient sound, leading to the observed $1/f$-like neuronal dynamics. To control for this possibility, we recorded the ambient sound in half of the rest sessions along with the neuronal data and compared the sound-wave amplitude modulations during rest and during audiovisual movie stimulation to the neuronal activity (Supplementary Fig. 3 online). Auditory electrodes showed substantial correlations with the movie soundtrack during stimulation (reflecting their auditory responsivity), whereas no such correlations were found between neuronal activity and ambient sound during rest ($r = -0.06$ and -0.16 for gamma-LFP and firing-rate modulations, respectively; $n = 6$ rest sessions comprising 38:22 min of data).

Comparing spontaneous and sensory-evoked activities

To determine the extent to which slow spontaneous fluctuations differ from sensory-evoked events, we compared the temporal dynamics of spiking activity during rest with those found in activity evoked by pure-tone and random-chord stimulation[22]. In particular, we checked whether the difference between sensory responses and spontaneous activity was evident in peak firing-rate amplitudes. We found that high firing rates (>20 spikes s^{-1}) measured over periods of 200 ms were significantly more frequent in stimulus-evoked than in rest activity ($P < 0.05$ by paired t test; Fig. 5a). For higher firing rates (>30 spikes s^{-1}), this difference was even more significant ($P < 3.1 \times 10^{-10}$ by paired t test). We also examined instantaneous peak firing rates during stimulation and rest as reflected in the interspike interval (ISI) distributions (Fig. 5b). The results again indicate that short ISIs (3–20 ms), reflecting high instantaneous firing rates, were much more prevalent during stimulus-evoked activity than during spontaneous activity. These differences indicate that, compared to stimulus-evoked responses, the spontaneous activity is mainly composed of relatively low-amplitude firing-rate modulations.

A straightforward prediction stemming from these different temporal dynamics is that the spectral profile of interhemispheric correlations during stimulus-evoked activity should be more uniform across different frequency bands compared to spontaneous activity—that is, a flat profile with a larger contribution of high frequencies, as in model 1 (Fig. 1). To examine this prediction, we computed the spectral profile of the interhemispheric correlations, as well as the power spectrum and cross-spectrum during chord stimulation, as we did for spontaneous activity (Figs. 3 and 4). The results show that high-frequency components of the correlated activity are indeed significantly enhanced in sensory-evoked responses compared to rest ($P < 0.05$ by t test; Supplementary Fig. 4 online).

Spatial selectivity of spontaneous fluctuations

An important property of large-scale spontaneous activity is its spatial selectivity; that is, distinct functional systems are often decorrelated in their rest activity. In the depth extracellular data, interhemispheric correlations between auditory cortices were indeed higher than correlations between the auditory cortex and other regions (Supplementary Fig. 5 online). The degree of spatial selectivity did not seem to be state dependent; in the one individual for whom sleep data were available, a quantitative comparison between wakeful rest and sleep states and slow, medium and fast frequencies did not reveal significant effects of state or speed on the spatial selectivity of correlations (two-way ANOVA on Fisher transformed selectivity indices, $P = 0.54$, $F > 0.62$ for state; $P = 0.67$, $F > 0.4$ for frequency; no interaction). However, these data were not optimal for assessing spatial selectivity, as many depth electrodes (apart from auditory cortex) were placed in subcortical sites (Supplementary Table 1). We therefore set

out to examine the spatial selectivity of spontaneous activity in additional individuals monitored with intracranial ECoG recordings (Supplementary Table 1), as such recordings provide a much better coverage of the cortical surface.

We first examined whether the basic findings of interhemispheric correlations were replicated in this group of individuals. To that end, we functionally identified auditory electrodes through their responses during audiovisual stimulation, which were highly correlated with movie soundtrack amplitude (see Methods and Supplementary Fig. 3 for details). For visually responsive electrodes, we followed our previous criteria[24] for identifying face-selective responses to the presentation of visual stimuli of various categories. Notably, some of the auditory and visual electrodes were also effective in eliciting corresponding precepts upon electrical stimulation conducted for clinical purposes (see Methods and Supplementary Table 2 online for details). Examining interhemispheric correlations between auditory electrodes revealed the following phenomena. First, concerning the raw LFP, we did not find robust correlations across hemispheres, although some variable correlations ($0.09 < r < 0.11$) were identified for theta and alpha oscillations (Supplementary Fig. 6 online). In contrast, unlike the depth electrodes, the raw LFP did show variable correlations between sites within the same hemisphere, but these correlations did not spread to the interhemispheric 'mirror' sites and were not consistent across the two individuals. Second, concerning BLP changes, we again found robust interhemispheric correlations in the gamma (>40 Hz) range ($r = 0.53$, $P < 0.0005$; Supplementary Fig. 6). Finally, concerning the spectral profile of gamma-power correlations, interhemispheric correlations were again more pronounced at low (<0.1 Hz) frequencies (Supplementary Fig. 6). Thus, the surface ECoG recordings largely manifested the same behavior for interhemispheric auditory correlations as did the extracellular depth recordings.

We then examined in detail the issue of spatial selectivity in spontaneous activity, as measured in ECoG gamma-power modulations. To that end, we calculated the correlation between the spontaneous activity of auditory or visual 'seed' electrodes and every other ECoG electrode (two individuals, $n = 106$ electrodes total; patient 4, Fig. 6; patient 5, Supplementary Fig. 7 online). In both individuals, interhemispheric correlations between corresponding mirror sites were significantly higher than correlations with nearly all other recording sites ($P < 0.05$ in 53 of 55 paired t tests). A quantitative examination (Fig. 6b,d) revealed a marked selectivity for functional networks, where interhemispheric correlations were robust between auditory cortices ($r = 0.61$) and between visual cortices ($r = 0.34$) but minimal across the two functional systems ($r = 0.02$).

Unlike the depth extracellular data, power changes in frequency bands of ECoG electrodes other than gamma showed strong correlations between recording sites (Supplementary Fig. 8 online). However, these correlations did not show consistent selectivity patterns. For example, alpha BLP showed extremely widespread and homogenous correlations across most of the sampled cortical surface (Supplementary Fig. 8). The observed difference between low-frequency power modulations in the depth recordings and intracranial surface ECoG data may be related to different spatial summation properties of the ECoG recording electrodes compared to the more localized depth extracellular recordings. Alternatively, it may reflect some heterogeneity in the level of alpha-power modulations across different recording sites.

We had so far focused our examination on the electrodes that showed the most pronounced and selective sensory-evoked responses. However, we also wanted to examine the extent to which the spatial selectivity phenomenon generalizes to other, less selective, sensory electrodes. To that end, we calculated all pairwise correlations between spontaneous gamma-power modulations recorded in sensory-related electrodes (all electrodes showing reproducible ($r > 0.2$) responses across repeated presentations of the audiovisual movie). We then plotted the relationship between such correlations and interelectrode distance from the mirror electrode

location expected in the other hemisphere (Supplementary Fig. 9 online). Although this analysis did not take into account potential neuroanatomical discontinuities and patchiness in functional networks, the results nevertheless revealed a trend for a decline in correlation with increasing interelectrode distance, reaching statistical significance in one individual ($P < 0.05$) and a nearly significant trend ($P = 0.068$) in the other individual (Supplementary Fig. 9).

Indirect comparison to spontaneous fMRI waves

Finally, to further evaluate the possibility that the neuronal activity recorded underlies spontaneous fMRI waves, we examined characteristics of the two phenomena that do not require simultaneous recordings, as these were unfeasible in the individuals studied. More specifically, we compared the magnitude and frequency profiles of interhemispheric correlations in the electrophysiological data and in fMRI data recorded in healthy subjects. To that end, we reanalyzed previously collected rest fMRI data[18] recorded in six subjects. We identified left and right auditory cortices anatomically and then sampled the time course of spontaneous activity for each subject. Data were filtered into slow (<0.1 Hz) and medium (>0.1 Hz) frequencies and compared separately across hemispheres. We found that the magnitude and frequency profiles of interhemispheric correlations were comparable to those observed in the electrophysiological data ($r = 0.67 \pm 0.17$ (mean ± s.d.) and 0.37 ± 0.15 for slow and medium frequencies, respectively). Correlations for slow waves were significantly greater than those observed for medium waves ($P = 0.009$ by paired t test). A detailed examination of faster fluctuations in fMRI data was not possible because of our magnetic resonance sampling frequency (0.33 Hz) and the inherent low-pass properties of the hemodynamic response function.

DISCUSSION

Modulations of spontaneous firing rate and gamma LFP power

Our results indicate the existence of spontaneous electrophysiological activity in the human sensory cortex that is significantly correlated across the two hemispheres. These correlations were robust during silent periods in wakeful rest and were markedly increased during sleep (Fig. 3). These results extend previous reports of very slow modulation of spontaneous neuronal activity[8,9] by revealing this activity in the human brain in both awake and sleep states, by showing its correlation between mirror sites across hemispheres, and by showing its functional selectivity. The coherent spontaneous waves were mostly evident in two components of the electrophysiological signals. First, and most important, they were evident in firing-rate modulations recorded in single neurons. Second, such fluctuations were found in power modulations of LFP gamma frequencies. As we have previously pointed out[25], it is important to distinguish between the broadband (40–100 Hz) gamma power changes that show correlated spontaneous fluctuations (and are well correlated to simultaneously recorded blood oxygen level–dependent fMRI[26]) and narrow-band (40 Hz) gamma oscillations, which are often associated with precise phase-locking phenomena[27] and do not necessarily correspond to the same physiological processes.

Given the very slow nature of spontaneous fluctuations, slow components of the raw LFP, such as delta or alpha waves, could have been expected to show similar cross-hemispheric correlations, as has been recently reported in anesthetized rats[28]. However, this was not revealed in our data, at least for frequencies >1 Hz.

Spontaneous fluctuations are dominated by low frequencies

A clear-cut aspect of the results is that spontaneous waves showing interhemispheric correlations were dominated by low-amplitude and very low temporal frequencies, following a 1/*f*-like power distribution. This was evident in the spectral profile of interhemispheric

correlations (Fig. 3a–d), in the power spectrum of local unilateral spontaneous activity and in the cross-spectrum of interhemispheric-correlated activity (Fig. 4).

Indirect support for the notion that long-distance correlations are dominated by slow activity modulations could also be derived when considering the correlation between spiking activity and gamma LFP (Supplementary Fig. 2). We recently proposed[25] that because the LFP measures the summed activity of large neuronal populations, the coupling between spiking activity of individual neurons and gamma LFP could be taken as an index for the distributed nature of the neuronal activity—that is, the extent to which single neurons modulate their firing rate in a coherent manner. Thus, strong spike-gamma coupling reflects widely distributed neuronal comodulation, whereas poor spike-gamma coupling reflects more heterogeneous and localized neuronal activity. Our present results showed that such spike-gamma coupling was stronger for the slow (<0.1 Hz) modulations (Supplementary Fig. 2). Taken together, these results suggest that widely distributed patterns of coactivation are dominated by slow modulations leading to strong spike-gamma coupling, whereas fast modulations are associated with localized islands of activity leading to poor spike-gamma coupling. This concept is compatible with our finding that interhemispheric correlations were most pronounced in slow activity modulations.

Potential confounding factors

The present results were obtained in individuals with epilepsy, who may have abnormal synchrony in their global activity patterns at the millisecond time resolution. However, this is unlikely to be the main source of the observed correlations for the following reasons. First, the auditory cortex was not identified as the epileptic focus in any of the individuals in this study. Second, interictal epileptiform events have markedly different temporal dynamics with extremely fast transients, and such epochs were identified and removed from the data. Third, the same neuronal population reported here showed ultrafine frequency tuning[22] and was tightly correlated to fMRI recordings in healthy subjects[25,29]. Finally, the spontaneous modulations we describe here showed remarkable selectivity for functional networks, whereas epileptiform events tend to be more global. We are therefore confident that the current results can be extended to the general population.

It could be argued that the observed correlated spontaneous activity in our study was actually sensory-driven by small background noises[30], as the experiments were not conducted in a soundproof room. However, after recording the ambient sound in half of the recording sessions, we found no correlations between neuronal activity and ambient sound during rest (Supplementary Fig. 3). The same correlated spontaneous fluctuations were observed in carefully controlled quiet periods as in our more typical recordings. Finally, the existence of interhemispheric correlations in the visual system (Fig. 6c,d), when the subject was resting with eyes closed, clearly argues against such an interpretation.

Spontaneous fluctuations manifest spatial selectivity

Spatial selectivity was expressed in the depth extracellular data as higher correlation between auditory cortices than between auditory cortex and other cortical sites (Supplementary Fig. 5). Notably, this spatial selectivity was maintained during REM and stage 2 sleep (Supplementary Fig. 5), although our data cannot resolve whether this was also the case during slow-wave sleep. The spatial selectivity of spontaneous activity was further confirmed and extended in the intracranial ECoG recordings, which allowed detailed mapping of the correlations across various cortical sites (Fig. 6). Furthermore, using a purely anatomical criterion, we found an overall trend for increased correlation in spatially similar electrode sites (Supplementary Fig. 9).

In the present study, we focused our analysis mainly on sensory-related electrodes. It is quite likely that spontaneous activity is not unique to the sensory cortex. However, there is a serious methodological difficulty in studying spontaneous activity in nonsensory areas, as it is difficult to control for unintentional task-related activations in such areas. As an example, consider activity in the motor cortex during rest. Unless detailed electromyography measurements are obtained, such activity may actually reflect slight involuntary motor actions. The underlying motor activity in the cortex could then either be correlated across hemispheres (for example, for bilateral movements) or may show a breakdown of interhemispheric correlation (for example, for unilateral motor acts). Such activations are difficult to disentangle from true spontaneous fluctuations.

Relation to human spontaneous fMRI fluctuations

Recent human fMRI studies revealed high-amplitude, widespread blood oxygen level–dependent fluctuations in the absence of sensory stimulation or behavioral tasks[12–19,21,31]. In sensory systems, such spontaneous fMRI fluctuations can often exceed the amplitude of a typical stimulus-driven perceptual event[18]. These spontaneous fluctuations are increasingly being used as a noninvasive tool for brain mapping in healthy and patient populations[21,32,33]. Notably, coherent spontaneous fMRI activity reflects the functional and anatomical organization of cortical networks and therefore serves as a powerful tool in the delineation of cortical and subcortical networks (see ref. [21] for review). Such delineation is typically achieved by searching for activity correlated with that found in a predefined 'seed' region of interest[12–16,18–21] (a procedure also termed functional connectivity), or by using data-driven methods such as clustering and independent-component analysis[17,34–36]. The spontaneous fluctuations often show high interhemispheric correlations between functionally related mirror sites[12–21]. Furthermore, these interhemispheric correlations have recently been shown to depend on intact callosal connections[37], thus indirectly supporting a neuronal origin for these waves.

Given this growing evidence for spontaneous fMRI activity, the role of firing-rate and gamma-power modulations reported here as the potential source of spontaneous fMRI fluctuations is of substantial interest. A definite answer requires simultaneous recordings of neuronal activity and fMRI in the human cortex, which are at present technically unfeasible. However, the spontaneous neuronal modulations reported here in fact match all the characteristics of spontaneous fMRI previously reported[21], including interhemispheric correlations across mirror sites, selectivity for functional networks and 1/*f*-like temporal dynamics. In addition, the coupling between gamma LFP power and fMRI has now been shown in a number of studies[24–26,29,38,39], including spontaneous activity in area V1 of anesthetized monkeys[40] (although it should be noted that the monkeys' eyes were mostly open during these recordings). Finally, our comparison of spontaneous fMRI dynamics in healthy volunteers with those found in electrophysiological patient data show a qualitative similarity, both in the magnitude and the spectral profile of interhemispheric correlations. Thus, it is likely that spontaneous modulations in firing rates and gamma power are the neuronal correlates of spontaneous fMRI fluctuations.

Dynamics of spontaneous and sensory-driven activities

Our results reveal clear differences in neuronal dynamics when comparing spontaneous to sensory-driven responses. Sensory responses showed significantly higher firing rates and shorter ISIs (Fig. 5). As to the duration of sensory-driven responses, although these were not the focus of the present study, a previous report analyzed the sensory response properties of these auditory neurons in detail and found relatively short (<200 ms) high-amplitude bursts of activity in response to chord stimulation (for example, Fig. 1 of ref. [22]). Similar auditory response dynamics were observed in monkey single-unit recordings[41,42]. Further support for

the fast transient dynamics of sensory-driven responses could be derived from our analysis of local and interhemispheric power spectra, which showed a relatively flat profile (Supplementary Fig. 4) similar to that suggested by model 1 (Fig. 1).

Taken together, these results point to a clear differentiation in the dynamics of sensory-driven and spontaneous activity corresponding to models 1 and 2 (Fig. 1), respectively. These marked differences in neuronal dynamics between spontaneous and sensory-driven activity may help resolve the apparent paradox of high-amplitude fMRI fluctuations emerging in the sensory cortex in the absence of an overt perceptual experience[18]. The current results suggest that high-amplitude rest fMRI fluctuations may be the result of the long integration time of the hemodynamic filter, which essentially amplifies slow neuronal activity modulations. Such temporal integration may cause low-amplitude rest activity (model 2) to seem comparable in fMRI signal magnitude to short-duration, high-amplitude sensory-evoked responses (model 1). This interpretation is fully compatible with models that posit high firing rates as a necessary condition for perceptual events[10,11]. Our data underscore the caution that must be exercised when interpreting the magnitude and dynamics of fMRI activations, especially those related to slow cognitive phenomena such as shifts in spatial attention[43].

Functional role of spontaneous activity

Spontaneous activity could in principle be related to consciously willful and intentional cognitive processes, such as imagery. However, our finding of a marked enhancement in interhemispheric correlations during sleep, especially in non-REM sleep stages (Fig. 3c,d), seems to argue against such a role. Alternatively, the functional role of spontaneous fluctuations may change across states and have a more cognitively meaningful role during wakefulness.

As to the function of the correlated spontaneous fluctuations, one intriguing option is that they serve some role in maintenance[44] and renormalization of synaptic contacts, as is suggested for slow-wave activity during sleep[45]. Such essentially random ‘maintenance’ activity, when driven through the hardwired neuroanatomical connectivity (for example, the corpus callosum), could result in the observed correlated fluctuations across interhemispheric mirror foci[46]. Another possibility is that spontaneously active networks with a balance of excitation and inhibition may respond more rapidly to inputs[47,48]. Future studies in which all cognitive aspects are carefully controlled (or largely absent, as in comatose individuals[49]) may help resolve this intriguing issue.

METHODS

Data acquisition

Neurophysiological recordings were obtained from five neurosurgical patients with pharmacologically intractable epilepsy, monitored for potential surgical treatment. Electrode location was based solely on clinical criteria. All individuals had electrodes placed bilaterally in or over the auditory cortex (Supplementary Table 1). All surgery was performed by I.F. Computed tomography scans after electrode implantation was coregistered to the preoperative MRI using iPlan Stereotaxy software (BrainLAB) to determine electrode positions. Individuals were required to provide written informed consent to participate in the experiments. This study conformed to the guidelines of the Medical Institutional Review Board at UCLA and at the Tel Aviv Sourasky Medical Center.

Extracellular depth recordings

Extracellular single-unit and LFP recordings were simultaneously obtained at UCLA from three individuals monitored with depth electrodes. Each electrode terminated in a set of nine

40-μm platinumiridium microwires. Signals were sampled at 28 kHz and bandpass-filtered in hardware between 1 and 9 kHz.

Electrocorticography surface recordings

Intracranial subdural ECoG recordings were obtained from two neurosurgical patients at Tel Aviv Medical Center. In total, 106 contact electrodes were examined (AdTech). ECoG data recordings were monopolar, referenced to an extracranial electrode, filtered electronically between 1 and 70 Hz and sampled at a rate of 200 Hz (Grass Technologies). Electrodes were placed directly on the cortical surface (2 mm diameter, 8 mm spacing between adjacent electrodes). Electrode locations (Fig. 6 and Supplementary Fig. 7) were projected on a reconstructed cortical surface of each individual using BrainVoyager software (Brain Innovation). As part of their clinical diagnostic routine, ECoG patients also participated in an electrical stimulation session and were asked to report their subjective perceptual experience immediately after such stimulation (see Supplementary Table 2 for subjective reports and Supplementary Methods online for technical details).

Experimental protocols

All experimental sessions were conducted after periods of at least 3 h without any identifiable seizures. Data from the same electrodes and individuals were collected during the wakeful rest, sleep and stimulation sessions described below.

Wakeful rest

We acquired wakeful rest data in 12 experimental sessions (on separate days) with five individuals (Supplementary Table 1). These recording sessions were conducted immediately before or after movie and chord stimulation sessions[22,24,25,29]. All sessions were conducted at the individuals' quiet bedside and lasted 392 ± 210 s (mean ± s.d.). During the rest sessions, subjects' eyes were closed, and the room was dark and quiet. In six of the rest sessions, the subject's task was passive ("close your eyes and relax"); in the other six sessions, we verified alertness by instructing subjects to press a keyboard button in response to a vocal instruction, once every 45 s on average. All intervals surrounding button presses or instructions were then removed from the rest dataset before the various analyses were conducted. For three of the five individuals (6 of 12 recording sessions), we digitally recorded the ambient sound in the room along with the neuronal data. These soundtracks were then used to identify and remove any time intervals that contained audible sounds and to conduct analysis of ambient sound during rest.

Sleep

We collected sleep data during two full nights from patient 2. Sleep was monitored by polysomnography, including two scalp EEG electrodes, electro-oculogram, chin electromyogram and video recording. Data were scored using international criteria[50]. Because the individual did not show persistent sleep (at least 5 min) in stages 3 and 4 of slow-wave sleep, all subsequent analysis was done on REM and stage 2 (non-REM) sleep segments.

Chord stimulation

Patients 2 and 3 (extracellular depth electrodes) were presented with a sequence of pure tones and random chords at a rate of 1 Hz for 1.5 and 3.5 min respectively, accompanied by random visual textures at a rate of 4 Hz, as recently described[22].

In addition, a visual object-category experiment and an audiovisual movie experiment were conducted in ECoG patients 4 and 5 to allow functional localization of auditorily and visually related electrodes for subsequent analysis of spontaneous activity.

Analysis of local field potentials and band-limited power

Preprocessing included the removal of 60 Hz (UCLA data) or 50 Hz (Tel Aviv data) and harmonics from the raw signals using a notch filter offline (MATLAB, Math-Works). Signals were then down-sampled to 1 kHz (UCLA data only). All data were further scanned manually for interictal epileptiform activity, and such time intervals were discarded from the dataset. Responses to stimuli recorded immediately before or after the rest sessions were highly correlated with fMRI responses in healthy individuals[24,25,29] and showed extremely sharp auditory and visual tuning characteristics[22,24], indicating that in general, our recordings were not significantly influenced by interictal epileptiform activity.

To examine raw LFP or BLP modulations at different frequency bands, we first used a second-order Butterworth filter (MATLAB) to apply zero-phase bandpass filtering to the raw LFP according to the following frequency bands: delta, 1–4 Hz; theta, 4–8 Hz; alpha, 8–14 Hz; low beta, 15–25 Hz; high beta, 25–40 Hz; gamma, 40–100 Hz. In the ECoG data (where data were filtered in hardware below 70 Hz), the gamma band was defined as 40–70 Hz. BLP modulations were extracted by applying full-wave rectification and smoothing as described previously[25]. Because all clinical recordings were high-pass filtered in hardware above 1 Hz, no information was available in the <1 Hz range.

Unit identification, cell selection and firing rates

In the analysis of the UCLA extracellular data, single units were identified with previous methodology[25,29]. The spike identification process was further validated by assessing the consistency of action potential waveforms and by verifying a clear spike refractory period (Fig. 5b). Example waveforms and distributions of ISIs for 32 units (taken from all microwires) are presented in Supplementary Figure 10 online.

The distribution (probability density function) of firing rates during rest and chord stimulation (Fig. 5a) was calculated as follows. The binary spike-train of each neuron was smoothed with a Gaussian with FWHM of 80 ms (which is nearly equivalent to binning the spikes into 200-ms bins with overlap) to extract a time course of instantaneous firing rates. The distribution of these firing rates was then calculated and averaged across neurons. The distribution of ISIs (Fig. 5b) was calculated separately for each neuron, averaged across different neurons and normalized so the area under the curve was equal to 1.

Correlation analyses

Correlations between left and right auditory cortices were examined separately for raw LFP and specific LFP frequencies (Fig. 4c and Supplementary Figs. 1 and 6), for BLP modulations (Figs. 2–4 and 6 and Supplementary Figs. 1 and 4–8) and for changes in the firing rates of local neuronal populations (Figs. 2–4). In the UCLA extracellular data, the signals of interest (LFP, BLP and firing rate) were extracted from each microwire and averaged across all microwires protruding from the same electrode (within ~3 mm) before interhemispheric correlations were computed. Firing-rate signals in these data were smoothed with a Gaussian with FWHM of 5 ms kernel to generate a continuous signal.

Next, BLP signals (extracellular data and ECoG data) and firing-rate signals (extracellular data only) were further filtered into slow (<0.1 Hz), medium (0.1–1 Hz) and fast (>1 Hz) fluctuations using a second-order, zero-phase Butterworth bandpass filter (MATLAB). Figures 2 and 6 and Supplementary Figures 3, 5, 7 and 9 show exclusively slow (<0.1 Hz) changes in LFP gamma power (gamma BLP) or firing rates. Supplementary Figure 8 shows slow (<0.1 Hz) changes in LFP power of all frequency bands. Figure 3 and Supplementary Figures 1, 2, 4 and 6 separately examine the independent contributions of slow, medium or fast fluctuations to interhemispheric correlations.

Correlations between full-band time courses of left and right auditory cortices in the UCLA extracellular data were also examined using standard cross-correlation (Fig. 4) as follows. We extracted the average neuronal firing rate and LFP gamma power in one hemisphere, computed the autocorrelation function or the interhemispheric cross-correlation function using standard techniques (MATLAB) and averaged these auto- or cross-correlation functions across sessions. The cross-spectrum (Fig. 4, insets) was extracted by applying a Fourier transform to the cross-correlograms.

Spatial topography in ECoG data

For the 'seed' analysis, spatial topography in ECoG data (Fig. 6 and Supplementary Fig. 7) was evaluated by computing the correlation between spontaneous changes in slow (<0.1 Hz) gamma BLP of auditory and visual seed electrodes and all other electrodes. The reliability of these spatial correlations was examined by dividing each recording into nonoverlapping, 120-s segments and computing the correlations to the seed electrode in each segment separately. Seed electrodes for 'functional connectivity' analysis during rest (Fig. 6c,d) in both ECoG patients were functionally identified by examining responses during audiovisual movie stimulation (auditory electrodes, see Supplementary Fig. 3), or using a standard visual object-category experiment[24] (visual electrodes).

For the pairwise analysis, we examined all interhemispheric correlations between pairs of sensory-related electrodes and the relation of such interhemispheric correlations to the proximity between electrodes (Supplementary Fig. 9).

Statistical analyses

Error bars, where present, denote s.e.m. between recording sessions conducted on different days or individuals (Fig. 3a,b and Supplementary Figs. 1 and 4–6); between separate, nonoverlapping data segments (Figs. 3c,d and 6b,d and Supplementary Figs. 1 and 5–8); between different neurons (Fig. 5); or between recording locations (Supplementary Fig. 2).

Significance values associated with Pearson correlation coefficients (asterisks in Fig. 3a–d and Supplementary Figs. 1 and 6) were assessed by comparing the real data (a collection of interhemispheric correlation coefficients) to a null distribution (a collection of random coefficients) using an unequal-variance Student *t* test on Fisher transformed coefficients (MATLAB). The null distribution was evaluated using a bootstrapping procedure by correlating spontaneous signals from left and right auditory cortices that were acquired at different times, providing an estimate of the random correlations expected for such signals.

Selectivity of interhemispheric correlations during wakeful rest (asterisks in Fig. 6b,d and Supplementary Figs. 5 and 7) was statistically tested by comparing the correlation coefficients between left and right auditory cortices to correlation coefficients between an auditory region and a different region, using a paired Student *t* test on Fisher transformed correlation coefficients. Comparisons between rest and stimulation firing-rate distributions (Fig. 5a) were conducted using a *t* test for each firing rate.

Additional details are provided in Supplementary Methods, including descriptions of fMRI acquisition and analysis, ECoG electrical stimulation sessions, visual object-localizer and audiovisual movie experiments, pairwise analysis of spatial correlations (Supplementary Fig. 9), spatial topography in UCLA data (Supplementary Fig. 5), interhemispheric correlation analyses for chord stimulation data (Supplementary Fig. 4), evaluation of possible asymmetry in cross-correlograms, analyses of ambient sound, ANOVA tests, bootstrapping procedure for generating null distributions and the exact interpretation of asterisks marking statistical significance in various figures.

Supplementary Material

Refer to Web version on PubMed Central for supplementary material.

Acknowledgements

We thank the participants for volunteering to take part in the study; A.D. Ekstrom, E. Isham, E. Ho, T.A. Fields, and E. Behnke for technical assistance at UCLA; C. Wilson and J. Ogren for help with sleep recordings and staging; D. Yossef, S. Nagar, R. Cohen, C. Yosef, G. Yehezkel and the EEG technicians for assistance at the Tel Aviv Medical Center; and R. Paz and E. Schneidman for helpful discussions and feedback. This study was funded by the Israel Science Foundation, Minerva and Benoziyo Center grants to R. Malach, a US-Israel Binational Science Foundation grant to I.F. and R. Malach and a Human Frontier Science Program Organization fellowship to R. Mukamel.

References

1. Llinas RR. The intrinsic electrophysiological properties of mammalian neurons: insights into central nervous system function. Science 1988;242:1654–1664. [PubMed: 3059497]
2. Arieli A, Sterkin A, Grinvald A, Aertsen A. Dynamics of ongoing activity: explanation of the large variability in evoked cortical responses. Science 1996;273:1868–1871. [PubMed: 8791593]
3. Kenet T, Bibitchkov D, Tsodyks M, Grinvald A, Arieli A. Spontaneously emerging cortical representations of visual attributes. Nature 2003;425:954–956. [PubMed: 14586468]
4. Leopold DA, Murayama Y, Logothetis NK. Very slow activity fluctuations in monkey visual cortex: implications for functional brain imaging. Cereb Cortex 2003;13:422–433. [PubMed: 12631571]
5. Laufs H, et al. Electroencephalographic signatures of attentional and cognitive default modes in spontaneous brain activity fluctuations at rest. Proc Natl Acad Sci USA 2003;100:11053–11058. [PubMed: 12958209]
6. Fiser J, Chiu C, Weliky M. Small modulation of ongoing cortical dynamics by sensory input during natural vision. Nature 2004;431:573–578. [PubMed: 15457262]
7. Mantini D, Perrucci MG, Del Gratta C, Romani GL, Corbetta M. Electrophysiological signatures of resting state networks in the human brain. Proc Natl Acad Sci USA 2007;104:13170–13175. [PubMed: 17670949]
8. Steriade M, Nunez A, Amzica F. A novel slow (<1 Hz) oscillation of neocortical neurons *in vivo*: depolarizing and hyperpolarizing components. J Neurosci 1993;13:3252–3265. [PubMed: 8340806]
9. Steriade M, Amzica F, Nunez A. Cholinergic and noradrenergic modulation of the slow (approximately 0.3 Hz) oscillation in neocortical cells. J Neurophysiol 1993;70:1385–1400. [PubMed: 8283204]
10. Grill-Spector K, Kushnir T, Hendler T, Malach R. The dynamics of object-selective activation correlate with recognition performance in humans. Nat Neurosci 2000;3:837–843. [PubMed: 10903579]
11. Kanwisher N. Neural events and perceptual awareness. Cognition 2001;79:89–113. [PubMed: 11164024]
12. Biswal B, Yetkin FZ, Haughton VM, Hyde JS. Functional connectivity in the motor cortex of resting human brain using echo-planar MRI. Magn Reson Med 1995;34:537–541. [PubMed: 8524021]
13. Lowe MJ, Mock BJ, Sorenson JA. Functional connectivity in single and multislice echoplanar imaging using resting-state fluctuations. Neuroimage 1998;7:119–132. [PubMed: 9558644]
14. Cordes D, et al. Mapping functionally related regions of brain with functional connectivity MR imaging. AJNR Am J Neuroradiol 2000;21:1636–1644. [PubMed: 11039342]
15. Greicius MD, Krasnow B, Reiss AL, Menon V. Functional connectivity in the resting brain: a network analysis of the default mode hypothesis. Proc Natl Acad SciUSA 2003;100:253–258.
16. Fox MD, et al. The human brain is intrinsically organized into dynamic, anticorrelated functional networks. Proc Natl Acad Sci USA 2005;102:9673–9678. [PubMed: 15976020]
17. Damoiseaux JS, et al. Consistent resting-state networks across healthy subjects. ProcNatl Acad Sci USA 2006;103:13848–13853.
18. Nir Y, Hasson U, Levy I, Yeshurun Y, Malach R. Widespread functional connectivity and fMRI fluctuations in human visual cortex in the absence of visual stimulation. Neuroimage 2006;30:1313–1324. [PubMed: 16413791]

19. Vincent JL, et al. Intrinsic functional architecture in the anaesthetized monkey brain. Nature 2007;447:83–86. [PubMed: 17476267]
20. Golland Y, et al. Extrinsic and intrinsic systems in the posterior cortex of the human brain revealed during natural sensory stimulation. Cereb Cortex 2007;17:766–777. [PubMed: 16699080]
21. Fox MD, Raichle ME. Spontaneous fluctuations in brain activity observed with functional magnetic resonance imaging. Nat Rev Neurosci 2007;8:700–711. [PubMed: 17704812]
22. Bitterman Y, Mukamel R, Malach R, Fried I, Nelken I. Ultra-fine frequency tuning revealed in single neurons of human auditory cortex. Nature 2008;451:197–201. [PubMed: 18185589]
23. Steriade M, McCormick DA, Sejnowski TJ. Thalamocortical oscillations in the sleeping and aroused brain. Science 1993;262:679–685. [PubMed: 8235588]
24. Privman E, et al. Enhanced category tuning revealed by intracranial electroencephalograms in high-order human visual areas. J Neurosci 2007;27:6234–6242. [PubMed: 17553996]
25. Nir Y, et al. Coupling between neuronal firing rate, gamma LFP and BOLD fMRI is related to interneuronal correlations. Curr Biol 2007;17:1275–1285. [PubMed: 17686438]
26. Logothetis NK, Pauls J, Augath M, Trinath T, Oeltermann A. Neurophysiological investigation of the basis of the fMRI signal. Nature 2001;412:150–157. [PubMed: 11449264]
27. Womelsdorf T, Fries P, Mitra PP, Desimone R. Gamma-band synchronization in visual cortex predicts speed of change detection. Nature 2006;439:733–736. [PubMed: 16372022]
28. Lu H, et al. Synchronized delta oscillations correlate with the resting-state functional MRI signal. Proc Natl Acad Sci USA 2007;104:18265–18269. [PubMed: 17991778]
29. Mukamel R, et al. Coupling between neuronal firing, field potentials and FMRI in human auditory cortex. Science 2005;309:951–954. [PubMed: 16081741]
30. Nelken I. Processing of complex stimuli and natural scenes in the auditory cortex. Curr Opin Neurobiol 2004;14:474–480. [PubMed: 15321068]
31. Mitra PP, Ogawa S, Hu X, Ugurbil K. The nature of spatiotemporal changes in cerebral hemodynamics as manifested in functional magnetic resonance imaging. Magn Reson Med 1997;37:511–518. [PubMed: 9094072]
32. Greicius MD, Srivastava G, Reiss AL, Menon V. Default-mode network activity distinguishes Alzheimer's disease from healthy aging: evidence from functional MRI. Proc Natl Acad Sci USA 2004;101:4637–4642. [PubMed: 15070770]
33. Liu H, et al. Decreased regional homogeneity in schizophrenia: a resting state functional magnetic resonance imaging study. Neuroreport 2006;17:19–22. [PubMed: 16361943]
34. Cordes D, Haughton V, Carew JD, Arfanakis K, Maravilla K. Hierarchical clustering to measure connectivity in fMRI resting-state data. Magn Reson Imaging 2002;20:305–317. [PubMed: 12165349]
35. Golland Y, Golland P, Bentin S, Malach R. Data-driven clustering reveals a fundamental subdivision of the human cortex into two global systems. Neuropsychologia 2008;46:540–553. [PubMed: 18037453]
36. Van de Ven VG, Formisano E, Prvulovic D, Roeder CH, Linden DE. Functional connectivity as revealed by spatial independent component analysis of fMRI measurements during rest. Hum Brain Mapp 2004;22:165–178. [PubMed: 15195284]
37. Johnston JM, et al. Loss of resting interhemispheric functional connectivity after complete section of the corpus callosum. J Neurosci 2008;28:6453–6458. [PubMed: 18562616]
38. Niessing J, et al. Hemodynamic signals correlate tightly with synchronized gamma oscillations. Science 2005;309:948–951. [PubMed: 16081740]
39. Nir Y, Dinstein I, Malach R, Heeger DJ. BOLD and spiking activity. Nat Neurosci 2008;11:523–524. [PubMed: 18437185]
40. Shmuel A, Leopold DA. Neuronal correlates of spontaneous fluctuations in fMRI signals in monkey visual cortex: Implications for functional connectivity at rest. Hum Brain Mapp 2008;29:751–761. [PubMed: 18465799]
41. Barbour DL, Wang X. Auditory cortical responses elicited in awake primates by random spectrum stimuli. J Neurosci 2003;23:7194–7206. [PubMed: 12904480]

42. Phan ML, Recanzone GH. Single-neuron responses to rapidly presented temporal sequences in the primary auditory cortex of the awake macaque monkey. J Neurophysiol 2007;97:1726–1737. [PubMed: 17135478]
43. Tootell RB, et al. The retinotopy of visual spatial attention. Neuron 1998;21:1409–1422. [PubMed: 9883733]
44. Fishbein I, Segal M. Miniature synaptic currents become neurotoxic to chronically silenced neurons. Cereb Cortex 2007;17:1292–1306. [PubMed: 16835294]
45. Tononi G, Cirelli C. Sleep function and synaptic homeostasis. Sleep Med Rev 2006;10:49–62. [PubMed: 16376591]
46. Morel A, Garraghty PE, Kaas JH. Tonotopic organization, architectonic fields and connections of auditory cortex in macaque monkeys. J Comp Neurol 1993;335:437–459. [PubMed: 7693772]
47. Tsodyks MV, Sejnowski T. Rapid state switching in balanced cortical network models. Network Comput Neural Syst 1995;6:111–124.
48. Vogels TP, Rajan K, Abbott LF. Neural network dynamics. Annu Rev Neurosci 2005;28:357–376. [PubMed: 16022600]
49. Laureys S, Boly M. What is it like to be vegetative or minimally conscious? Curr OpinNeurol 2007;20:609–613.
50. Rechtschaffen, A.; Kales, AA. A Manual of Standardized Terminology, Techniques, and Scoring System for Sleep Stages of Human Subjects. US Department of Health, Education and Welfare; Bethesda, Maryland: 1968.

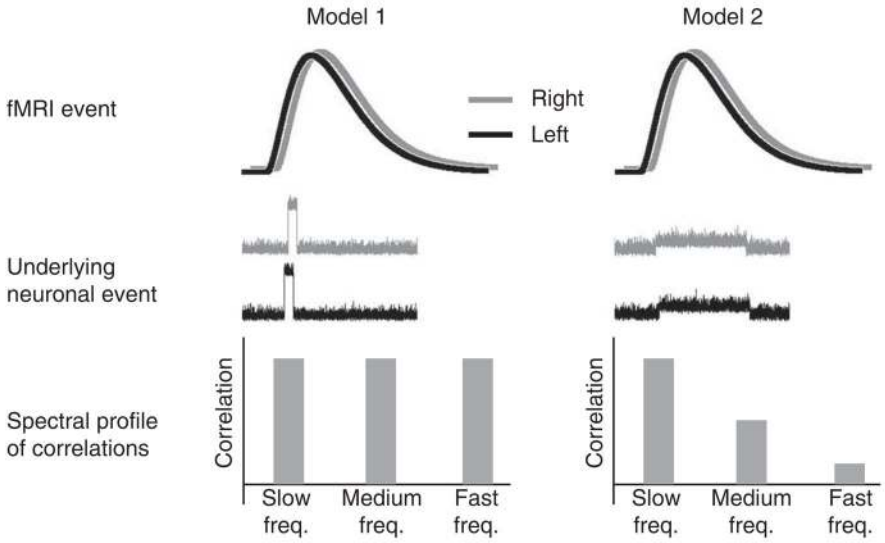

Figure 1.

Two models of possible neuronal activity underlying fMRI events. Correlated fMRI fluctuations from right (gray) and left (black) hemispheres (top row) could be generated by different underlying neuronal events (middle row) associated with different power spectra of interhemispheric correlations (bottom row). Model 1 (left column): fMRI activation generated by transient (~100–300 ms), high-firing-rate neuronal events. Model 2 (right column): fMRI activation generated by slow (on the order of seconds), low-firing-rate neuronal events. Both neuronal events include noise and temporal jitter. Fast neuronal events (model 1) would show interhemispheric correlations in all frequencies, whereas slow neuronal events (model 2) would show interhemispheric correlations predominantly in low frequencies (bottom row). Because of the temporal integration of the hemodynamic response, both neuronal dynamics could generate similar fMRI fluctuations (top row).

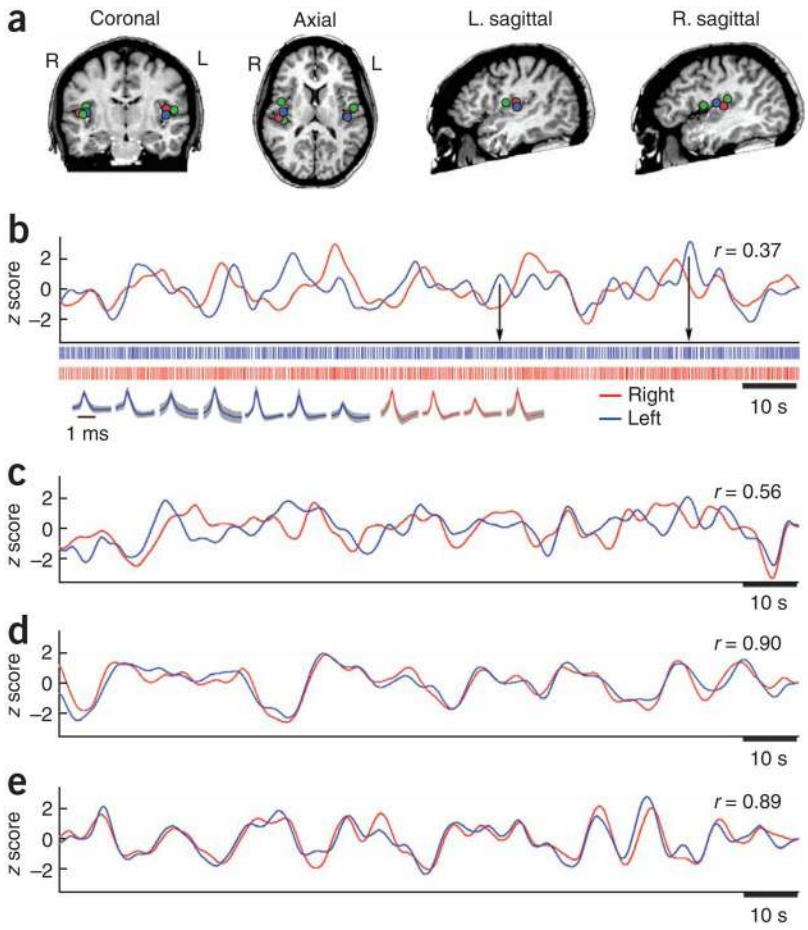

Figure 2.

Interhemispheric comparison of slow spontaneous activity in human auditory cortex. (**a**) Estimated anatomical locations of auditory electrodes in patients 1–3 (red, blue and green, respectively). (**b**–**e**) Examples of correlated slow fluctuations (<0.1 Hz) in neuronal activity of auditory cortex from the right (red) and left (blue) hemispheres. **b**, Firing-rate modulations during rest. Vertical lines show actual spike times. Black arrows indicate the relation between time courses of slow firing-rate modulations and actual spikes. Waveforms of neuronal action potentials are shown below spike trains (blue, left hemisphere; red, right hemisphere; gray zone, s.e.m. across spike instances). (**c**) LFP gamma-power modulations during wakeful rest. (**d**) LFP gamma-power modulations during REM sleep. (**e**) LFP gamma-power modulations during stage 2 sleep. Data in all examples were recorded in the same microwires of patient 2. Slow modulations tend to correlate across hemispheres, and correlations were markedly enhanced during sleep.

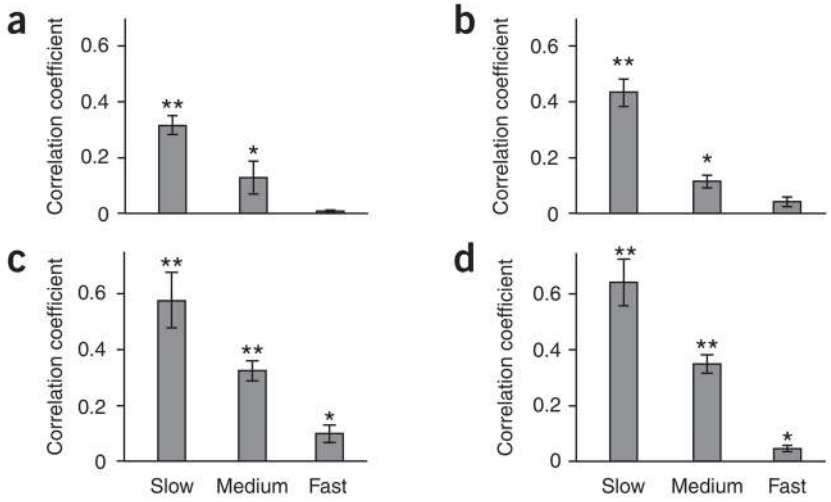

Figure 3.

Profiles of correlated spontaneous activity. Spectral distributions of interhemispheric correlations are shown in **a**–**d** for firing-rate and gamma-power modulations. Histograms show fast (>1 Hz), medium (0.1–1 Hz) and slow (<0.1 Hz) fluctuations. *$P < 0.05$ relative to null distribution assessed by bootstrapping (*t* test); **$P < 0.0005$. Error bars denote s.e.m. between recording sessions (wake) or recording segments (sleep). (**a**) Correlations in neuronal firing rates during wakeful rest ($n = 8$ recording sessions comprising 38:47 min of data in two individuals). (**b**) Correlations in LFP gamma power during wakeful rest ($n = 12$ recording sessions comprising 78:27 min of data in five individuals). (**c**) Correlations in LFP gamma power during REM sleep ($n = 17$ recording segments comprising 85 min of data in one individual). (**d**) Correlations in LFP gamma power during stage 2 sleep ($n = 13$ recording segments comprising 65 min of data in one individual). Low-frequency bias was observed in all correlations of interest, in agreement with model 2 (Fig. 1).

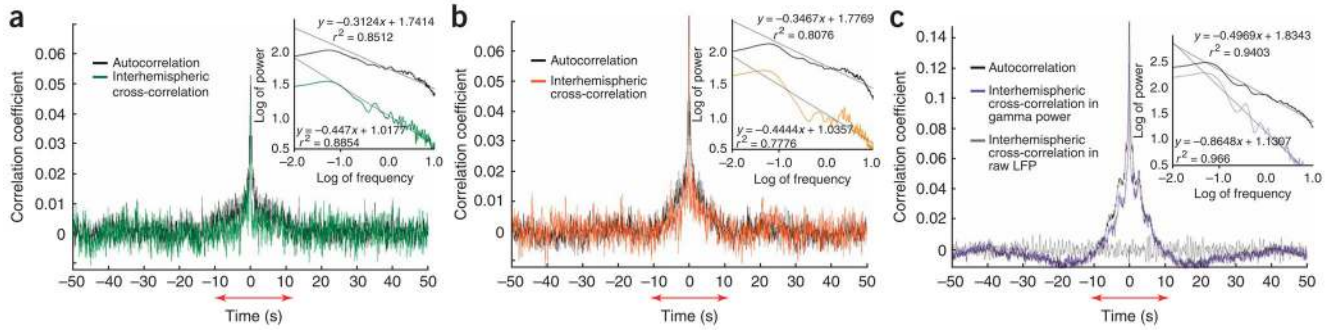

Figure 4.

Cross- and autocorrelograms. Cross- and autocorrelation functions of signals from left and right auditory cortices. (**a**) Cross- and autocorrelations of neuronal firing rates during wakeful rest ($n = 8$ recording sessions comprising 38:47 min of data in two individuals). Green, cross-correlation; black, autocorrelation. Red arrows indicate very slow elevation in correlation (±10 s) corresponding to very slow correlated fluctuations <0.1 Hz. Inset shows Fourier transform of cross- and autocorrelation functions (cross-spectrum and spectrum, respectively) showing 1/*f*-like distributions. (**b**) Cross- and autocorrelations of LFP gamma power during wakeful rest ($n = 9$ recording sessions comprising 49:07 min of data in three individuals). Orange, cross-correlation; black, autocorrelation. Inset as in **a**. (**c**) Cross- and autocorrelations of LFP gamma power during REM and stage 2 sleep ($n = 30$ recording segments comprising 150 min of data in one individual). Purple, cross-correlation; black, autocorrelation; gray, raw LFP above 1 Hz. Raw LFP, in which no correlations were found across hemispheres, is markedly different from gamma-power changes showing robust correlations. Inset and red arrows as in **a**. For all panels, *y* axis is truncated around peak levels of cross-correlation, whereas autocorrelation reaches 1 at lag zero (data not shown).

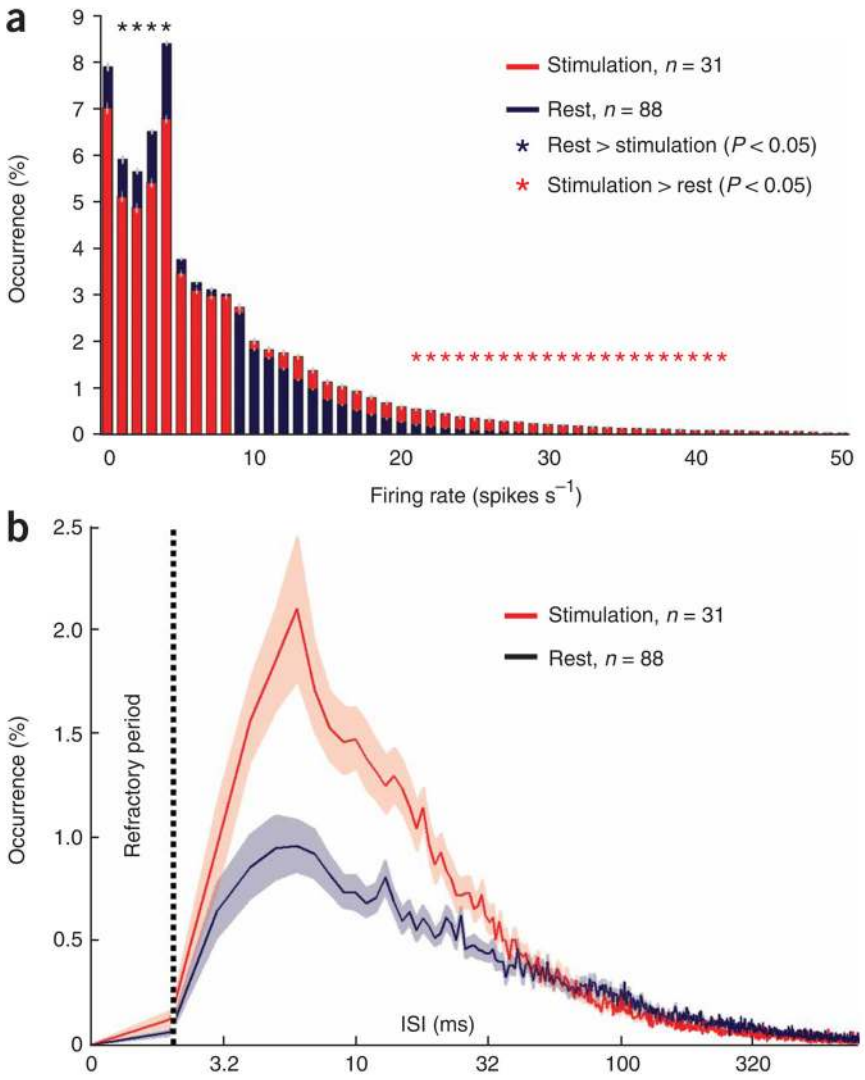

Figure 5.

Firing-rate and ISI distributions during rest and stimulation. (**a**) Distribution of firing rates during auditory stimulation and spontaneous activity. Gray bars mark s.e.m. across neurons. Low firing rates (1–4 spikes s^{-1}) were significantly more frequent during rest, whereas high firing rates (>20 spikes s^{-1}) were significantly more frequent during stimulation, in accordance with model 1 (Fig. 1). (**b**) ISI distributions during auditory stimulation and spontaneous activity. *x* axis is shown on a log scale. Area left of dotted line shows 1- to 2-ms interval for which no such ISIs were found, reflecting the spike refractory period indicative of single-unit recordings. Shaded areas denote s.e.m. across neurons. Short ISIs (3–20 ms), reflecting bursts of high firing rates, were more frequent during stimulation (model 1 in Fig. 1) than during rest (model 2 in Fig. 1).

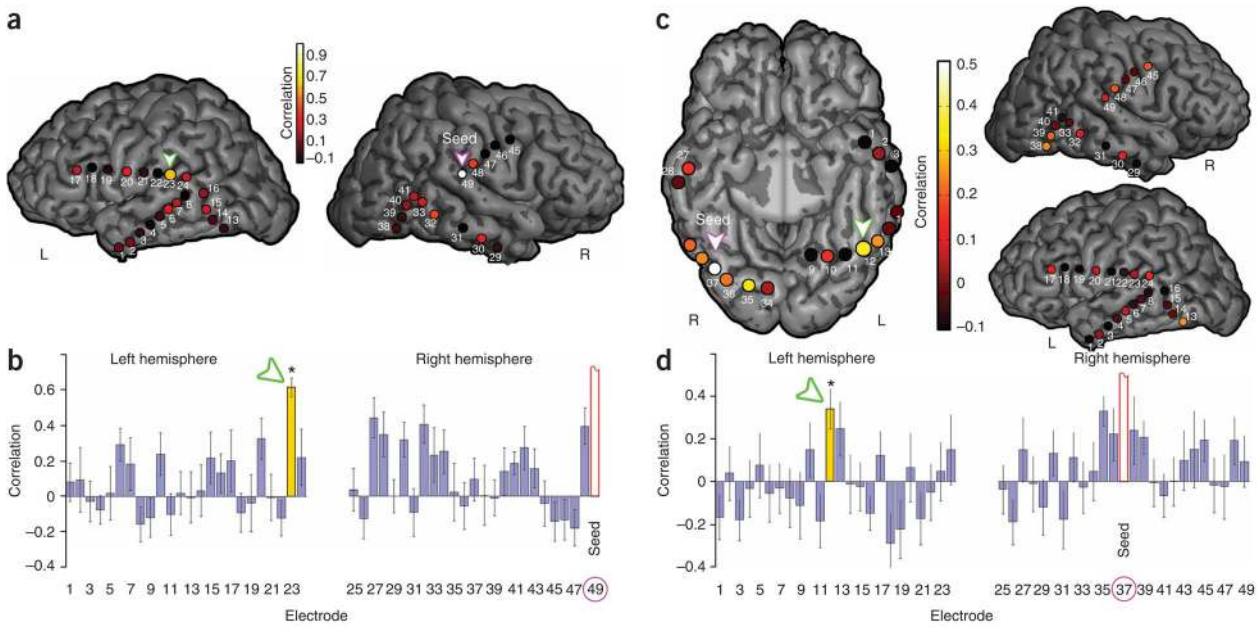

Figure 6.

Spatial topography of spontaneous correlations in intracranial ECoG data. (**a**) Correlations between slow spontaneous changes (<0.1 Hz) in ECoG gamma power of an auditory-related electrode of patient 4 ('seed', purple arrow, 49) and all other electrodes. Results are shown on a cortical reconstruction of the individual's brain as seen from a lateral view. Color of electrodes denotes their correlation with the seed electrode's activity. The strongest correlation in the left hemisphere (green arrow, 23) is found in a corresponding anatomical location. (**b**) Strength and variability of correlations with auditory seed electrode (purple circle, 49). Bars show mean correlations ± s.e.m. between nonoverlapping 2-min data segments. **P* <0.05 (*t* test) compared to all other electrodes in the left hemisphere. (**c**) Correlations between slow spontaneous changes (<0.1 Hz) in ECoG gamma power of a visual-related electrode of the same individual ('seed', purple arrow, 37) and all other electrodes. Results shown using a ventral view (left) and lateral view (right). The strongest correlation in the left hemisphere (green arrow, 12) is found in a corresponding anatomical location. Minimal correlation was observed between visual and auditory electrodes, indicating the functional selectivity of spontaneous correlations. (**d**) Strength and variability of correlations with visual seed electrode (purple circle, 37). **P* < 0.05 (*t* test) compared to all other electrodes except for adjacent electrode 13.